Molecular Modeling of Saccharides, Part 21[+]

Solution Geometries and Lipophilicity Patterns of α-Cycloaltrin**

Stefan Immel, Kahee Fujita, and Frieder W. Lichtenthaler*[a]

Abstract: Detailed analysis of the conformational features of α-cycloaltrin (**1**) in aqueous solution by temperature dependent ^{1}H and ^{13}C NMR studies, together with molecular dynamics simulations, reveal that the six altropyranose units are in a complex dynamic equilibrium within the $^4C_1 \rightleftharpoons {}^OS_2 \rightleftharpoons {}^1C_4$ pseudorotational turntable. This gives rise to a large number of macrocyclic conformations, ranging from a disk-shaped molecule with a hydrophobic central hole (alternating $^4C_1/^1C_4$ form **1a**) to a torus form of the macrocycle with an equally hydrophobic throughgoing cavity (all skew-boat form **1b**). Constrained MD simulations throw light on the conformational transitions between these two extreme forms (**1a** $\rightleftharpoons$ **1b**). Flexure of one altropyranoid chair into the skew-boat-$^OS_2$ form forces adjoining altropyranoid units to follow suit, thereby eliciting a successive, synergistic "rolling around" within the, on average, elliptical macrocycle. Thus, α-cycloaltrin is the first thoroughly flexible cyclooligosaccharide and can be used to probe the induced-fit mode of guest–host interactions.

Keywords: α-cycloaltrin · cyclodextrins · lipophilicity patterns · molecular dynamics · molecular modeling · solution geometries

Introduction

Research towards cyclooligosaccharides made from sugar units other than glucose[2–11] has been undertaken throughout the last decade. The foremost incentive in this pursuit is the generation of molecular receptors with recognition features different from those of the well-studied, overly rigid cyclodextrins (CDs). Unfortunately, only the inulin-derived[3a] cyclofructins with six and seven $\beta(1\rightarrow2)$-linked fructofuranose units became accessible in quantities sufficiently large to demonstrate their ability to complex metal cations.[12] The guest-complexation behavior of all other non-glucose cyclooligosaccharides could only be assessed by molecular modeling studies. Those composed of D-mannose (α- and β-cyclomannin[4]) and L-rhamnose (α-cyclorhamnin[5]), or both,[9] have their axially oriented 2-OH group directed towards the outside of the macrocycle, as evident from the contact surface and cross section plot for α-cyclomannin (Figure 1). A somewhat smaller torus height than in α-cyclodextrin results, yet this has no principal effect on the backbone structure, the cavity dimensions, or the lipophilicity pattern.[6, 10] A similar α-CD-like geometry was found for a cyclogalactin consisting of six $\beta(1\rightarrow4)$-linked galactopyranose residues (Figure 1, top right), yet its lipophilicity profile is different because hydrophobic surface regions at the primary hydroxyl face are substantially enlarged.[6]

More profound changes in shape, cavity dimensions, and guest-binding properties are to be anticipated for cyclooligosaccharides with axially disposed 3-OH groups in their pyranoid rings, since these 3-OH groups are directed towards the interior of the cavity. As illustrated in Figure 1 for the hexameric α-cycloallin, steric congestion resulting therefrom induces the allopyranose units to adopt a wide range of tilt angles relative to the macrocycle and a substantial narrowing of the 2-OH/3-OH side of the torus, yet the pyranoid $^4C_1$ geometries are retained without exception.[14]

For cyclic oligosaccharides composed of D-altropyranoses—those with six (α-cycloaltrin **1**[11]), seven,[7] and eight $\alpha(1\rightarrow4)$-linked units[8] have recently become accessible from

[a] Prof. Dr. F. W. Lichtenthaler, Prof. K. Fujita,[+] Dr. S. Immel
Institut für Organische Chemie, Technische Universität Darmstadt
Petersenstrasse 22, D-64287 Darmstadt (Germany)
Fax: (+49) 6151-166674
E-mail: fwlicht@sugar.oc.chemie.tu-darmstadt.de

[+] Permanent address:
Faculty of Pharmaceutical Sciences, Nagasaki University
Nagasaki 852-8131 (Japan)

[+] Presented in part at the XIXth International Carbohydrate Symposium, San Diego (USA), August 1998; Abstract A124. Part 20: K. Fujita, W.-H. Chen, D.-Q. Yuan, Y. Nogami, T. Koga, T. Fujioka, K. Mihashi, S. Immel, F. W. Lichtenthaler, *Tetrahedron: Asymmetry* **1999**, *10*, 1689–1696.

[**] A cyclooligosaccharide composed of six $\alpha(1\rightarrow4)$-linked D-altropyranose residues; for derivation of the terminology used see ref. [1]

Supporting information for this article in the form of 3D structures of Figure 1 and MOLCAD graphics is available on the WWW under http://caramel.oc.chemie.tu-darmstadt.de/immel/3Dstructures.html and http://caramel.oc.chemie.tu-darmstadt.de/immel/molcad/gallery.html, respectively.

  0947-6539/99/0511-3185 $ 17.50+.50/0

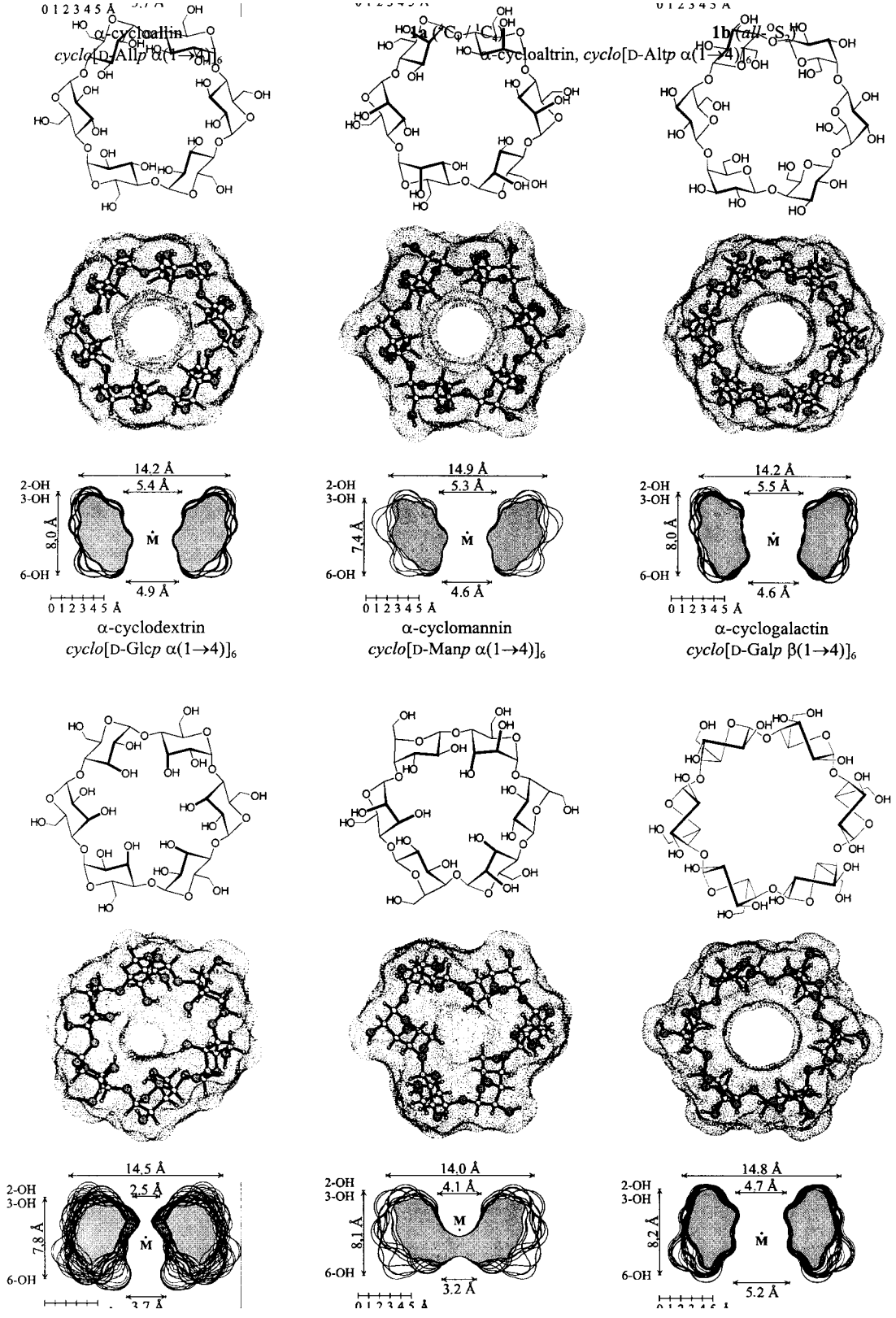

Figure 1. Molecular geometries of α-cyclodextrin[13] compared to cyclooligosaccharide analogues composed of six identical hexopyranose residues in their macrocycle: D-mannose (α-cyclomannin[6]), D-galactose (α-cyclogalactin[6]), D-allose (α-cycloallin[14]), and D-altrose (α-cycloaltrin, in its solid-state form **1a** and the *all*-skew-$^{O}S_2$ geometry **1b** emerging from HTA simulations as the global minimum energy structure[10, 11]). Conventional chemical formulas (top entries), calculated contact surfaces (in dotted form with ball-and-stick-model insert, center), and cross-section plots with approximate molecular dimensions (2-OH and 3-OH sides up) are depicted.

0947-6539/99/0511-3186 $ 17.50+.50/0 *Chem. Eur. J.* **1999**, *5*, No. 11

the respective cyclodextrins in a high-yielding four-step procedure—retention of the $^4C_1$ geometry for the altropyranoid rings (with axially disposed 2-OH and 3-OH groups) is highly unlikely, since there is ample calculatory[15] and ^{1}H NMR evidence[16] that α-D-altropyranose itself and a variety of its simple derivatives establish a dynamic equilibrium within the $^4C_1 \rightleftharpoons {}^1C_4$ pseudorotational "turntable" (Figure 2). X-ray crystallography revealed that α-cycloaltrin

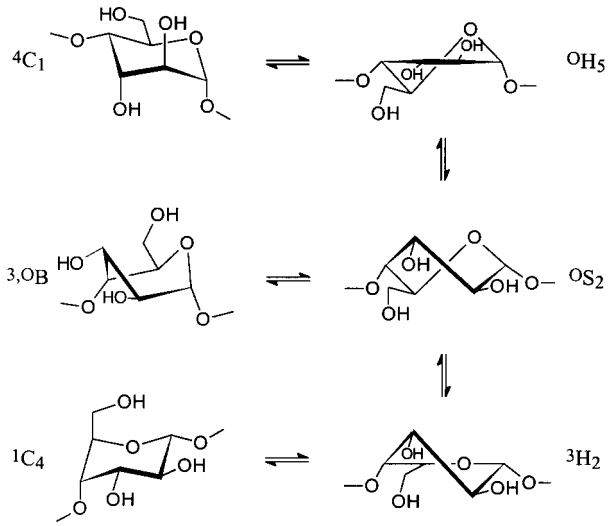

Figure 2. The chair/half-chair/skew (twist-boat) pseudorotational itinerary between α-D-altropyranoid rings in $^4C_1$ and $^1C_4$ conformation. The $^{3,O}B$ and $^OS_2$ forms are closely related to each other, hence have similar coupling constants and are not differentiated in Table 1 and Figure 4; the two half-chair conformations $^OH_5$ and $^3H_2$ appear to be higher in energy and are transition states in the $^4C_1 \rightleftharpoons {}^1C_4$ conformational itinerary.

adopts an architecturally unprecedented macrocyclic structure comprising an alternating sequence of $^4C_1$ and $^1C_4$ pyranoid chair conformations, resulting in a disk-shaped molecule with a central indentation rather than a through-going cavity (Figure 1, **1a**).[11] This unique topography in the solid state, in spite of being embedded into a matrix of 21 water molecules, does not survive on dissolution in water, for only one set of ^{1}H NMR signals are observed.[11] This finding is compatible with either of the following two scenarios: operation of a dynamic equilibrium between the $^4C_1$ and $^1C_4$ chairs within the pseudorotational transitions illustrated in Figure 2, whereby NMR measurements average over the variety of macrocyclic conformations, or alternatively, adoption of a fixed conformation, an *all*-skew (twist-boat) form conceivably, as this form emerges from high-temperature annealing (HTA) simulations as the global energy minimum structure (**1b** in Figure 1). Notably, this *all*-$^OS_2$ form **1b** contains a cavity that is larger and possesses the opposite conicity than that of α-cyclodextrin, and **1b** should therefore be able to form inclusion complexes with sterically matching guests.

A detailed study towards a differentiation between these possibilities appeared warranted since—should a dynamic equilibrium prevail in solution—the cycloaltrins would be the first thoroughly flexible cyclooligosaccharides capable of adapting their overall geometries to binding of appropriate guests, a process that more closely corresponds to Koshland's induced-fit mode of substrate-receptor interaction[17] than to the overly static lock-and-key model.[18] These issues are herein explored by temperature-dependent NMR analysis, standard and constrained MD simulations, and generation of the lipophilicity patterns of the closed and open forms **1a** and **1b**.

Results and Discussion

Temperature-dependent NMR analysis: High-resolution ^{1}H and ^{13}C NMR spectra of α-cycloaltrin (**1**) in D_2O (Figure 3) display only one set of signals for the six altropyranoses, indicating either fast averaging between different altropyranoid ring conformations, or alternatively adoption of a uniform geometry somewhere in between the $^4C_1$ and $^1C_4$ conformation for all six altrose units. Experimental ^{1}H NMR coupling constants (Table 1) are consistent with either scenario.

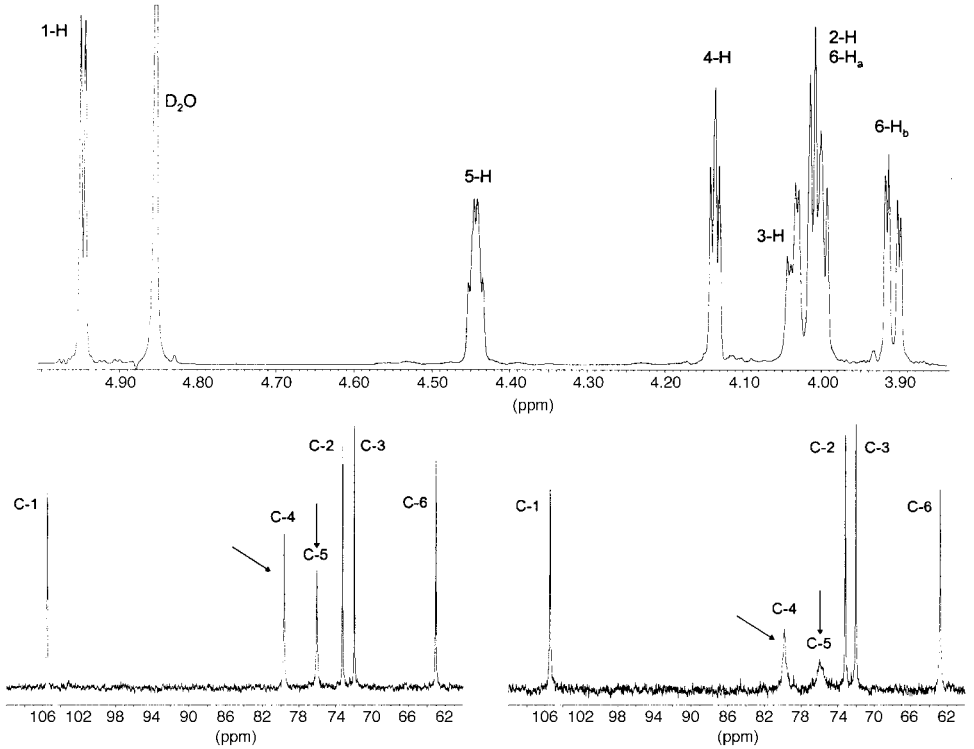

Figure 3. Top: 800 MHz ^{1}H NMR spectrum of α-cycloaltrin (**1**) in D_2O at 30 °C reveals one set of signals. Bottom: 200 MHz ^{13}C NMR spectra of **1** in D_2O at 32 °C (left) and 4 °C (right). As indicated by the arrows, the signals of C-4 and C-5 are significantly broadened at lower temperatures.

  0947-6539/99/0511-3187 $ 17.50+.50/0

Table 1. Comparison of the altropyranoid ring ^{1}H-^{1}H-coupling constants for α-cycloaltrin (800 MHz, D_2O, 30 °C) with those calculated for its $^4C_1$, $^1C_4$, and all-$^OS_2$ (skew) forms.

		Calculated[a] for			
$J_{H,H}$ [Hz]	Found	$^4C_1$[b]	$^1C_4$[b]	$^OS_2$[c]	$^4C_1/^1C_4/^OS_2$[d]
$J_{1,2}$	4.73	2.2	8.0	4.0	4.9
$J_{2,3}$	8.19	2.7	10.2	10.2	8.3
$J_{3,4}$	3.71	3.4	2.4	4.5	3.5
$J_{4,5}$	5.32	9.7	1.4	6.4	5.5

[a] Calculation based on the Karplus-type H–C–C–H torsion angle dependency of coupling constants, including the electronegativity effect to the substitution pattern by use of the generalized Haasnoot equation.[19] [b] Values obtained for the pyranose conformations realized in the crystal structure **1a**. [c] Data resulting from calculations on the HTA-derived global energy minimum *all*-skew form **1b**.[10, 11] [d] Least-squares fit for 26% $^4C_1$, 34% $^1C_4$, and 40% $^OS_2$, roughly corresponding to a 1:1:1 mixture of conformers.

The presence of a dynamic conformational equilibrium in aqueous solution is inferred from the temperature dependence of the ^{1}H NMR data: the value for $J_{2,3}$ decreases from 8.2 Hz at 30 °C to 7.6 and 7.1 Hz at 20 and 4 °C, respectively, thereby narrowing the well-separated signal for H-3. Although the smaller value of $J_{2,3}$ at 4 °C suggests a more intensely populated $^4C_1$ altrose conformation in the $^4C_1 \rightleftharpoons {}^OS_2 \rightleftharpoons {}^1C_4$ pseudorotational itinerary, the best fit of calculated[19] versus measured coupling constants emerging from the triangle representation of Figure 4, revealed a composition of 26% $^4C_1$, 34% $^1C_4$, and 40% $^OS_2$ (cf. center minimum of σ-contours at 0.18 Hz), indicating, within the margin of error, the presence of essentially equal proportions of the three forms.

More profound temperature effects are observed for the ^{13}C signals of C-4 and C-5, which are substantially broadened on lowering the temperature from 30 to 4 °C (cf. Figure 3). This is clearly indicative of a dynamic equilibrium of various altropyranoid geometries which starts to "freeze out" at 4 °C. However, the NMR data neither reveal which of the many macrocyclic conformations within the sterically limiting "straitjacket" of **1** are preferred, nor answer the question of how the conformational transitions **1a** ⇌ **1b** occur.

Molecular dynamics simulations: MD simulations with explicit incorporation of the (aqueous) solvent were performed for both α-cycloaltrin forms, **1a** and **1b**. Despite considerable flexibility in the macrocycles, no significant conformational transitions for the pyranose units were observed within a time frame of 600 ps (Figure 5). The solute hydration shells can be readily characterized from these calculations. An average of 30.6 ± 2.7 and 39.6 ± 3.4 water molecules are hydrogen-bonded to **1a** and **1b**, respectively. Any change of the altropyranose conformations entails substantial rearrangements in this tightly bound first hydration shell, rendering these processes too slow to be observable during standard MD simulations. The crucial role of water in the rearrangement process becomes particularly evident when comparing the MDs in solution with HTA simulations on α-cycloaltrin in vacuum: at high (1200 K) as well as at low temperatures (300 K) frequent and unhindered conformational transitions are observed for the altrose units in the isolated macrocycle.

The effects on the macrocycle of changing a $^4C_1$ altrose unit in the $^4C_1/^1C_4$ form **1a** along the $^4C_1 \rightarrow {}^OS_2 \rightarrow {}^1C_4$ pathway can be monitored within a reasonable nanosecond time frame by means of constrained MD techniques: two pyranose ring torsion angles O_5–C_1–C_2–C_3 and C_3–C_4–C_5–O_5 of one altrose unit are restrained in such a way that the $^4C_1$ conformation is forced to vary in the desired direction (Figure 6, gray shaded altrose residue **B**). As this ring flip is artificially induced, the neighboring unconstrained monosaccharide units—each in the $^1C_4$ form—are subject to considera-

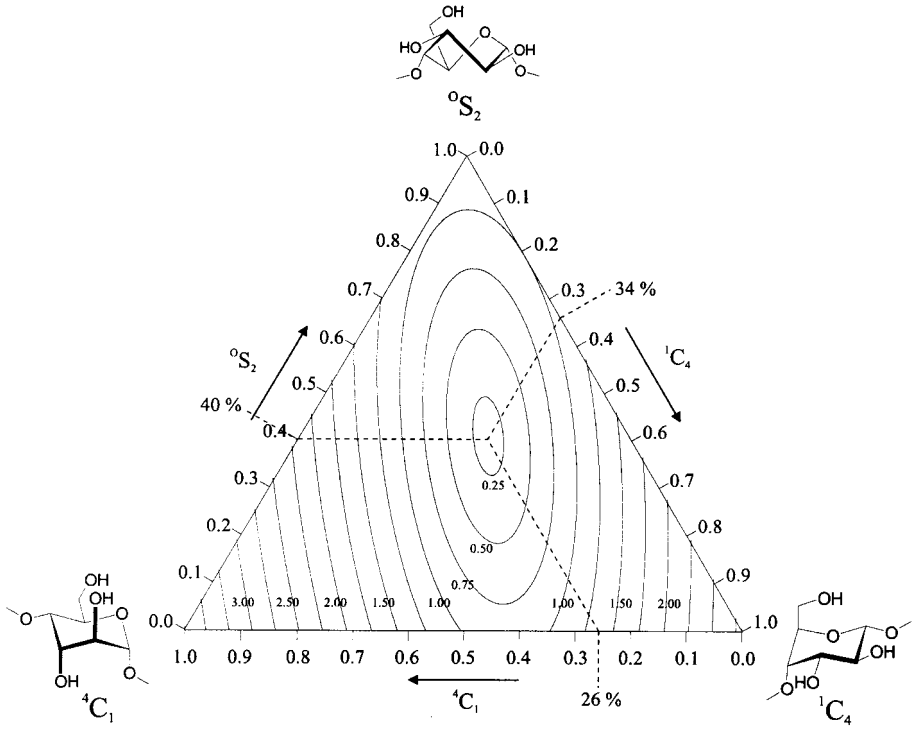

Figure 4. Triangular contour plot of the root-mean-square deviation (i.e. the error σ) of the calculated pyranose ring coupling constants ($J_{1,2}$, $J_{2,3}$, $J_{3,4}$, and $J_{4,5}$) versus those found experimentally. Contours are given as a function of the altrose conformational equilibrium between $^4C_1$ (left corner of the triangle), $^1C_4$ (right), and $^OS_2$ forms (top corner), and are plotted at levels of σ = 0.25 to 4.00 Hz in 0.25 Hz steps; the triangle axes are in units of molecular fractions $\chi_i = 0.0 - 1.0$. The $^3J_{H,H}$ coupling constants for the pure $^4C_1$, $^1C_4$, and $^OS_2$ pyranose forms (triangle corners) were obtained from the solid-state structure and the minimum-energy geometry of **1**. The values are listed in Table 1. The best-fit of calculated versus experimental data (center minimum of the σ-contours at $\sigma_{min} = 0.18$ Hz) emerged for 26% $^4C_1$, 34% $^1C_4$, and 40% $^OS_2$ (equilibrium composition marked by hatched lines); all other mixtures yielded larger errors.

0947-6539/99/0511-3188 $ 17.50+.50/0 *Chem. Eur. J.* **1999**, *5*, No. 11

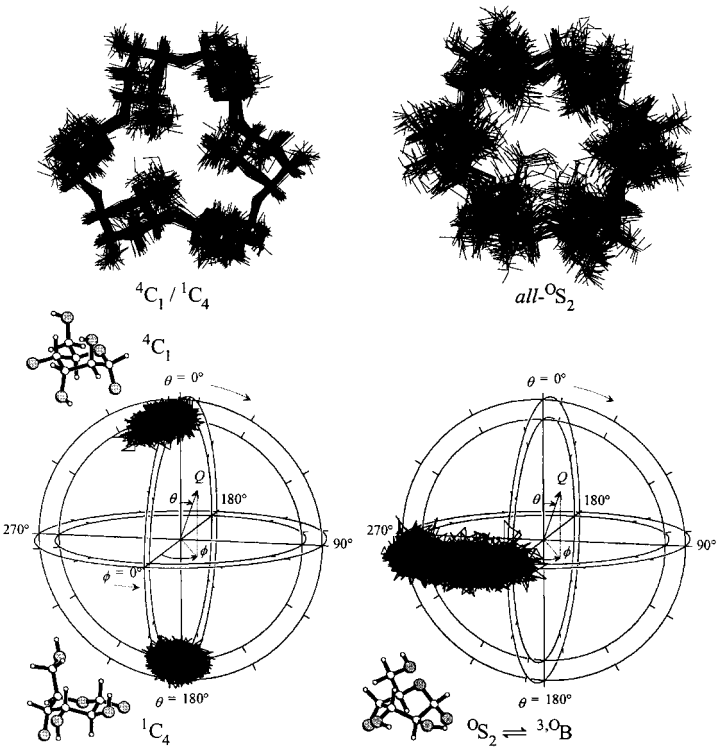

Figure 5. Top: Superimpositions of 60 α-cycloaltrin snapshot geometries taken in 10 ps intervals from MD simulations of **1a** (left) and **1b** (right) in water illustrate the flexibility of the macrocycles, despite relative conformational rigidity of the pyranose rings. Bottom: Polar-coordinate plots of the pyranose Cremer–Pople ring-puckering parameters[28] derived from MD simulations of **1a** (left plot, solid-state structure) and **1b** (right, HTA-derived start geometry) in water. In both cases a time series (trajectory) of the pyranose puckering parameters Q, ϕ and θ is plotted in 3D-polar coordinates (height, longitude, and latitude): On the left, the well-separated trajectories for the $^4C_1$ and $^1C_4$ altrose units lack any conformational transitions between the different chair geometries within the MD time frame of approximately 600 ps; similarly, **1b** displays no significant deviations from the $^OS_2 \leftrightarrow {}^{3,O}B$ geometries during the entire MD simulation.

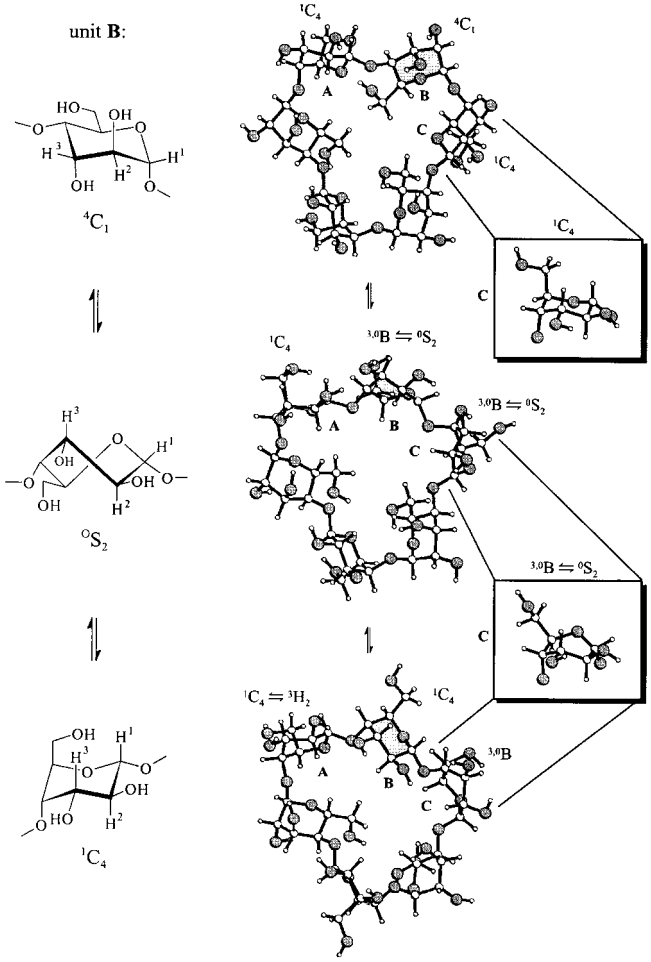

Figure 6. Constrained MD simulations of α-cycloaltrin exhibit a conformational transition of the central $^4C_1$ altropyranose (gray-shaded unit **B**) of a $^1C_4$-$^4C_1$-$^1C_4$-fragment (units **A**-**B**-**C**) in the macrocycle: as **B** is driven along the $^4C_1 \rightarrow {}^{3,O}B/{}^OS_2 \rightarrow {}^1C_4$ reaction coordinate (formulas, left column), the conformation of the neighboring residue **A** varies very little with slight distortions $^1C_4 \rightarrow {}^3H_2$ only, but the altrose unit **C** cooperatively flips into a $^{3,O}B \rightleftharpoons {}^OS_2$ geometry (zoomed structures on the right). The unperturbed and cooperative conformational transitions of adjacent pyranose units point towards complex dynamic processes, in the course of which altrose residues cannot be considered independent; each conformational change induces new strains in neighboring units (all α-cycloaltrin snapshot structures were taken from a 130 ps MD perturbation, and constraints were applied to unit **B** only).

ble intrinsic strain in the macro-ring: one is only slightly distorted towards the half-chair form ($^1C_4 \rightarrow {}^3H_2$, unit **A** in Figure 6), whereas the residue on the other side (**C**) displays a full transition along $^1C_4 \rightarrow {}^OS_2 \rightleftharpoons {}^{3,O}B$. As this ring-flip was not induced by additionally applied MD potentials, it reveals the way conformational changes occur within the macrocycle: flexure of one altropyranoid chair into the intermediate skew-$^OS_2$ form via half-chair transition states forces the two adjoining altrose chairs, tied up in a macrocyclic "straitjacket" type clamp, to follow suit, and so on, thereby eliciting a consecutive "rolling around" in the probably elliptically distorted macrocycle.

As the above mechanism for interconversion involves energy concentration on one altrose unit (the restrained residue) with consecutive geometry changes in the macrocycle, there might be an alternative transition pathway: structural changes through excitation of low-energy macromolecular vibrational modes by thermal collisions with the solvent. Although such a mode of interconversion is difficult to induce through constrained MDs and was not observed during the standard MD simulations, it cannot be ruled out entirely. However, the question of whether structural changes in the macrocycle induce transitions in the monomers or vice-versa is bound to remain open as both conformational motions seem to be so intricately interwoven to the extent of being inseparable.

In either case, the overall result is a statistical scrambling over the $^4C_1$, $^OS_2$, and $^1C_4$ forms for the six altropyranose residues, of which the NMR data (Figure 3 and Table 1) provide an averaged picture. Although the distinct forms **1a** and **1b** cannot be identified directly from the NMR data presented in Figures 3 and 4, they should be taken into account as limiting structures in this complex conformational equilibrium.

Molecular lipophilicity patterns: Generation of molecular lipophilicity patterns (MLP)[20] of the solid-state conformation

1a[11] and of the HTA-derived energy-minimum *all*-$^{O}S_2$ form **1b**[10, 11] was achieved by the MOLCAD program,[21] and was projected[22] in color-coded form onto their contact surfaces[23] depicted in Figure 1. The results displayed in Figure 7 allow a first assessment of the inclusion-complexation capabilities of α-cycloaltrin. Both the disk- (**1a**) and torus-shaped form (**1b**) reveal a distinct front–rear differentiation of hydrophobic and hydrophilic surface regions. The 2-OH, 3-OH side—in analogy to the cyclodextrins[6, 10]—turns out to be the most hydrophilic part of the molecule, in contrast to a significantly more hydrophobic reverse side owing to the primary 6-CH_2OH groups. Although **1a** lacks a central "through-going" cavity, this conformer has a hydrophilic surface indentation and an outer core made up of irregularly distributed hydrophilic and hydrophobic regions (Figure 7, top right). In contrast, the cyclodextrin-like, torus-shaped form **1b** displays a more uniform pattern of the corresponding surface qualities (Figure 7, bottom): the most hydrophobic surface areas extend from the 6-CH_2OH side well into the cavity, yet the tilt of the pyranose units in the macrocycle is the inverse of that present in α-cyclodextrin (Figure 1, top left).

Conclusion

These results provide unambiguous insight into the solution geometries of α-cycloaltrin (**1**) and into the comparable stabilities of the $^{4}C_1$- and $^{1}C_4$-chair forms of its altropyranose residues. A large variety of macrocyclic shapes are possible within the constraints of its cyclohexasaccharide "straitjack-

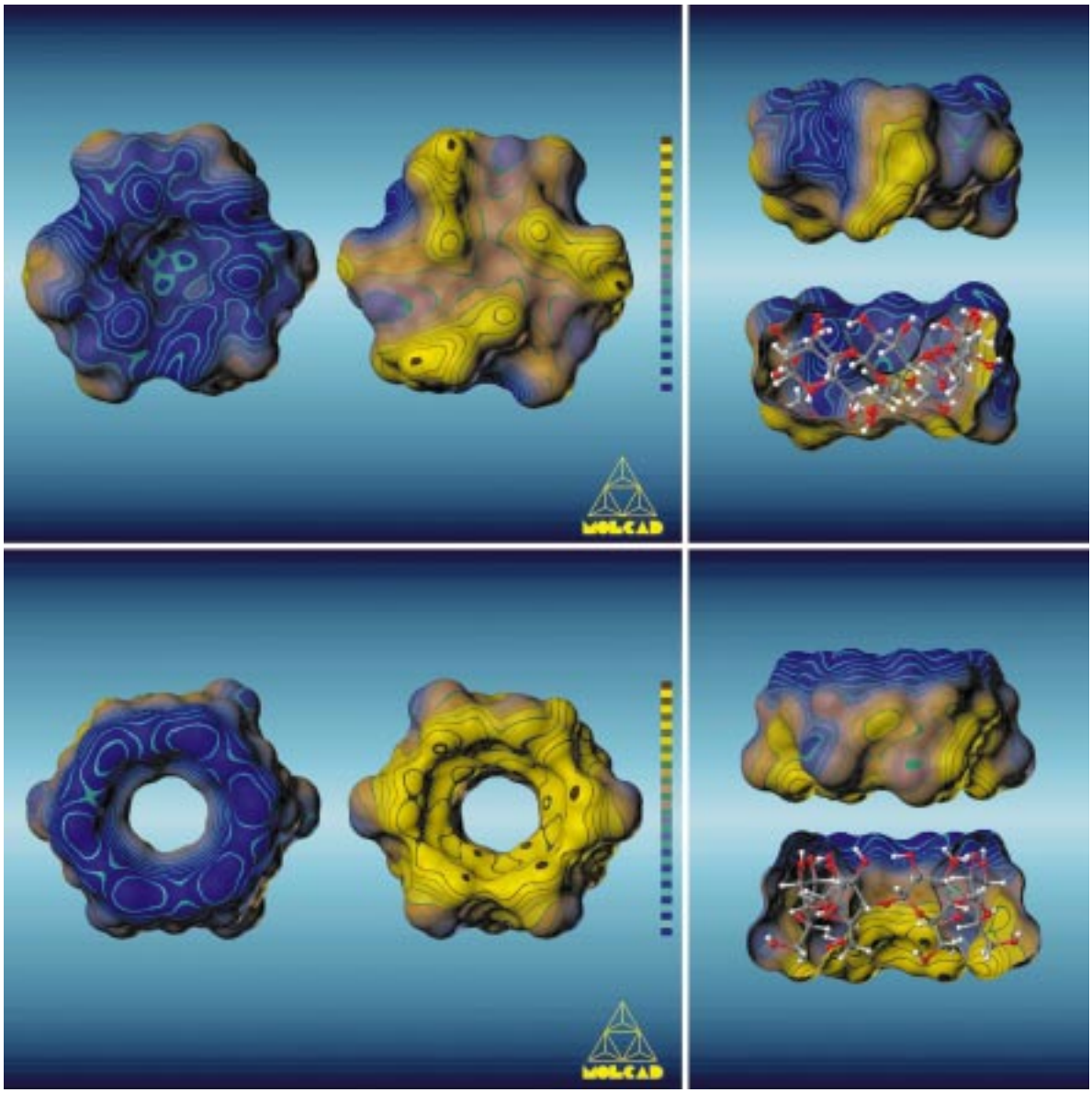

Figure 7. Molecular lipophilicity patterns of α-cycloaltrin (**1**) projected onto the contact surfaces of the solid-state conformation (**1a**, top) and the *all*-$^{O}S_2$ form (**1b**, bottom). The color code applied ranges from dark blue for the most hydrophilic surface areas to full yellow corresponding to the most hydrophobic regions. On the left, the macrocycles are viewed from both sides perpendicular to the mean ring plane, exposing either the pronouncedly hydrophilic (blue) 2-OH/3-OH side of the torus or the opposite, hydrophobic rim made up from the primary 6-CH_2OH hydroxyl groups. The graphics on the right display the corresponding side views in closed and bisected form each, with the 2-OH and 3-OH groups directed upwards and the CH_2OH moieties at the lower rim.

0947-6539/99/0511-3190 $ 17.50+.50/0 *Chem. Eur. J.* **1999**, *5*, No. 11

et". The shapes range from a disk-shaped macrocycle with a distinctly hydrophobic central hole, which is realized when the pyranose units adopt an alternating sequence of $^4C_1$ and $^1C_4$ conformations (**1a**), to a torus shape with an equally hydrophobic through-going cavity, realized when all pyranoid rings are in the skew-boat-$^OS_2$ form (**1b**). Both forms are limiting structures of a complex dynamic equilibrium. Accordingly, α-cycloaltrin (**1**) constitutes *the first thoroughly flexible cyclooligosaccharide* with which to realistically probe the induced-fit mode[17] of guest–host interactions. All previous utilizations of the overly rigid cyclodextrins as artificial enzymes[24] have only served as models for the stationary lock-and-key type[18] of enzyme action.

First evidence from capillary electrophoresis studies indicates that α-cycloaltrin and 4-*tert*-butylbenzoate form inclusion complexes. We hope that a sufficiently large number of guests interacting with α-cycloaltrin will justify broad exploration of this system.

Experimental Section

Temperature-dependent ^{1}H (800 MHz) and ^{13}C (200 MHz) spectra were recorded at the "Large Scale Facility for Biomolecular NMR" of the University of Frankfurt.

HTA[10, 11] and MD calculations were carried out using the CHARMM[25] force field for carbohydrates[26] and application of periodic boundaries (MDs, truncated octahedron filled with 606 (**1a**) and 611 (**1b**) water molecules, box size approximately 32 Å), isothermal ($T = 300$ K), and isobaric conditions ($p = 1$ bar) during a simulation time of 600 ps (equilibration time 25 ps, time step 1 fs); analysis of the MD trajectories was accomplished with external computer programs.[27]

Constrained MD computations of α-cycloaltrin (cf. Figure 6) were carried out using the isothermal and isobaric simulation system as described above. Starting from the solid-state conformation **1a**, the ring torsion angles O_5–C_1–C_2–C_3 (Θ_1) and C_3–C_4–C_5–O_5 (Θ_4) of one altropyranose unit were constrained and driven during 39 independent MD runs with steps of 3° each, forcing one $^4C_1$ altrose geometry to vary slowly into the inverted $^1C_4$ conformation (*"reaction parameters"* Θ_1: $+57° \rightarrow -57°$, Θ_4: $-57° \rightarrow +57°$). Each MD trajectory was carried out for a 10 ps equilibration and a 25 ps data acquisition period, the final structures were used as a starting point for the next MD run after re-setting the torsion angles to the new values along the reaction coordinate. The conformational transitions of the remaining five unconstrained altrose residues were monitored by use of Cremer–Pople parameters.[28]

Calculation of the molecular contact surfaces and the respective hydrophobicity potential profiles[20] was performed by using the MOLCAD[21] molecular modeling program and its texture mapping option.[22] The MLP profiles were scaled in relative terms (most hydrophilic to most hydrophobic surface regions) for each molecule separately; no absolute values are displayed.

The minimum-energy structure of α-cycloallin was derived from a 675 ps MD study in water (CHARMM force field,[25, 26] $T = 300$ K, $p = 1$ bar, 609 water molecules, parameters as above), with subsequent full energy minimization of a total of 13248 isolated solute structures by application of the PIMM91 force field,[29] which is particularly suitable for carbohydrate structures without solvent.

Least-squares fitting of the J values for three conformations $^4C_1$, $^1C_4$, and $^OS_2$ was achieved with root-mean-square deviations of $\sigma_J = 0.18$ Hz, whereas a two-state model $^4C_1 \rightleftharpoons {}^1C_4$ yielded $\sigma_J = 0.80$ Hz.

Acknowledgements

We are grateful for financial support from Fonds der Chemischen Industrie, Frankfurt, and for a fellowship (to K.F.) from the Deutscher Akademischer Austauschdienst, Bonn, In addition, we thank Prof. Dr. C. Griesinger and Dr. H. Schwalbe, Goethe Universität Frankfurt, for recording the ^{1}H (800 MHz) and ^{13}C (200 MHz) NMR spectra, and Prof. Dr. J. Brickmann, Institut für Physikalische Chemie, Technische Universität Darmstadt, for providing access to his MOLCAD software package.

[1] a) The naming of non-glucose cyclooligosaccharides, in particular of those composed of different sugar units, can be exasperating. According to recent IUPAC Recommendations (*Carbohydr. Res.* **1997**, *297*, 78 ff.), the systematic name for **1** turns out to be *cyclohexakis-(1→4)-α-*D*-altropyranosyl*, implying that **1** represents a assembly of "glycosyls" rather than being a "glycoside". In fact it is a hexasaccharide. Alternatively the semi-systematic name *cyclo-α(1→4)-*D*-altro-hexaoside*, abbreviated as "*cyclo*[D-Alt*p* $\alpha(1\rightarrow4)]_6$", may be used, based on a recent proposal for a simplified nomenclature,[1b, 6] which has been authoritatively endorsed.[1c] The most simple and practical designation, however—at least for cyclooligosaccharides with a single type of sugar unit—is inferred from traditional CD terminology (dextrose being an old name for glucose), syllogistically leading to "cycloaltrin" and the Greek letters α, β, and γ designating the respective species with six, seven, and eight hexose units. Accordingly, **1** is appropriately termed *α-cycloaltrin*,[11] and the next higher homologues, *β*-[7] and *γ-cycloaltrin*.[8] Correspondingly, other known non-glucose cyclooligosaccharides with one type of monosaccharide unit are reasonably named *α-*, *β-*, and *γ-cyclomannin*,[4, 6] *α-cyclorhamnin*,[5] and *α-* and *β-cyclofructin*.[3] b) S. Immel, J. Brickmann, F. W. Lichtenthaler, *Liebigs Ann. Chem.* **1995**, 929–942; c) J. Szejtli, in *Comprehensive Supramolecular Chemistry*, *Vol. 3 (Cyclodextrins)*, (Eds.: J. Szejtli, T. Osa), Pergamon, Oxford, UK, **1996**, pp. 7 ff.; J. Szejtli, *Chem. Rev.* **1998**, *98*, 1743–1753.

[2] L. V. Backinowsky, S. A. Nepogodiev, N. K. Kochetkov, *Carbohydr. Res.* **1989**, *185*, C1–C3; L. V. Backinowsky, S. A. Nepogodiev, N. K. Kochetkov, *Tetrahedron* **1990**, *46*, 139–150.

[3] a) M. Kawamura, T. Uchiyama, T. Kuramoto, Y. Tamura, K. Mizutani, *Carbohydr. Res.* **1989**, *192*, 83–90; b) M. Sawada, T. Tanaka, Y. Takai, T. Hanafusa, T. Taniguchi, M. Kawamura, T. Uchiyama, *Carbohydr. Res.* **1991**, *217*, 7–17; c) S. Immel, F. W. Lichtenthaler, *Liebigs Ann. Chem.* **1996**, 39–44; d) S. Immel, G. E. Schmitt, F. W. Lichtenthaler, *Carbohydr. Res.* **1998**, 313, 91–105.

[4] M. Mori, Y. Ito, T. Ogawa, *Carbohydr. Res.* **1989**, *192*, 131–146; M. Mori, Y. Ito, J. Uzawa, T. Ogawa, *Tetrahedron Lett.* **1990**, *31*, 3191–3194.

[5] a) M. Nishizawa, H. Imagawa, Y. Kan, H. Yamada, *Tetrahedron Lett.* **1991**, *32*, 5551–5554; *Synlett* **1992**, 447–448; b) M. Nishizawa, H. Imagawa, E. Morikuni, S. Hatekayama, H. Yamada, *Chem. Pharm. Bull.* **1994**, *42*, 1356–1365.

[6] F. W. Lichtenthaler, S. Immel, *Tetrahedron: Asymmetry* **1994**, *5*, 2045–2060.

[7] K. Fujita, H. Shimada, K. Ohta, Y. Nogami, K. Nasu, *Angew. Chem.* **1995**, *107*, 1783–1784; *Angew. Chem. Int. Ed. Engl.* **1995**, *34*, 1621–1622.

[8] Y. Nogami, K. Fujita, K. Ohta, K. Nasu, H. Shimada, C. Shinohara, T. Koga, *J. Inclusion Phenom. Mol. Recognit. Chem.* **1996**, *25*, 53–56.

[9] P. R. Ashton, C. L. Brown, S. Menzer, S. A. Nepogodiev, J. F. Stoddart, D. J. Williams, *Chem. Eur. J.* **1996**, *2*, 580–591.

[10] F. W. Lichtenthaler, S. Immel, *J. Inclusion Phenom. Mol. Recognit. Chem.* **1996**, *5*, 3–16.

[11] Y. Nogami, K. Nasu, T. Koga, K. Ohta, K. Fujita, S. Immel, H. J. Lindner, G. E. Schmitt, F. W. Lichtenthaler, *Angew. Chem.* **1997**, *109*, 1987–1991; *Angew. Chem. Int. Ed. Engl.* **1997**, *36*, 1899–1902.

[12] a) N. Yoshie, H. Hamada, S. Takada, Y. Inoue, *Chem. Lett.* **1993**, 353–356; b) T. Uchiyama, M. Kawamura, T. Uragami, H. Okuno, *Carbohydr. Res.* **1993**, *241*, 245–248.

[13] F. W. Lichtenthaler, S. Immel, *Liebigs Ann. Chem.* **1996**, 27–37.

[14] S. Immel, G. E. Schmitt, unpublished results.

[15] a) S. J. Angyal, *Aust. J. Chem.* **1968**, *21*, 2737–2746; b) M. K. Dowd, A. D. French, P. J. Reilly, *Carbohydr. Res.* **1994**, *264*, 1–19.

[16] F. W. Lichtenthaler, S. Mondel, *Carbohydr. Res.* **1997**, *303*, 293–302.

[17] D. E. Koshland, Jr., *Angew. Chem.* **1994**, *106*, 2368–2372; *Angew. Chem. Int. Ed. Engl.* **1994**, *33*, 2375–2378.

[18] a) E. Fischer, *Ber. Dtsch. Chem. Ges.* **1894**, *27*, 2985–2993; b) F. W. Lichtenthaler, *Angew. Chem.* **1994**, *106*, 2456–2467; *Angew. Chem. Int. Ed. Engl.* **1994**, *33*, 2364–2374.

  0947-6539/99/0511-3191 $ 17.50+.50/0

[19] C. A. G. Haasnoot, F. A. A. M. DeLeeuw, C. Altona, *Tetrahedron* **1980**, *36*, 2783 – 2792.
[20] W. Heiden, G. Moeckel, J. Brickmann, *J. Comput.-Aided Mol. Des.* **1993**, *7*, 503 – 514.
[21] a) J. Brickmann, *MOLCAD - MOLecular Computer Aided Design*, Darmstadt University of Technology, **1996**; *J. Chem. Phys.* **1992**, *89*, 1709 – 1721; b) J. Brickmann, T. Goetze, W. Heiden, G. Moeckel, S. Reiling, H. Vollhardt, C.-D. Zachmann, *Interactive Visualization of Molecular Scenarios with the MOLCAD/SYBYL Package*, in *Data Visualization in Molecular Science: Tools for Insight and Innovation* (Ed.: J. E. Bowie), Addison – Wesley, Reading, MA **1995**, pp. 83 – 97.
[22] M. Teschner, C. Henn, H. Vollhardt, S. Reiling, J. Brickmann, *J. Mol. Graphics* **1994**, *12*, 98 – 105.
[23] M. L. Connolly, *J. Appl. Crystallogr.* **1983**, *16*, 548 – 558.
[24] a) R. Breslow in *Inclusion Compounds*, *Vol. 3* (Eds.: J. L. Atwood, J. E. D. Davies, D. D. MacNicol), Academic Press, London, **1984**, pp. 473 – 508; M. Komiyama, H. Shikegawa in *Comprehensive Supramolecular Chemistry*, *Vol. 3* (Eds.: J. Szejtli, T. Osa), Pergamon, Oxford, **1996**, pp. 401 – 422; b) R. Breslow, S. D. Dong, *Chem. Rev.* **1998**, *98*, 1997 – 2011.
[25] B. R. Brooks, R. E. Bruccoleri, B. D. Olafson, D. J. States, S. Swaminathan, M. Karplus, "CHARMM: A program for macromolecular energy, minimization, and dynamics calculations" in *J. Comp. Chem.* **1983**, *4*, 187 – 217.
[26] S. Reiling, M. Schlenkrich, J. Brickmann, *J. Comput. Chem.* **1996**, *17*, 450 – 468.
[27] S. Immel, *MolArch*$^+$ *– MOLecular ARCHitecture Modeling Program*, Darmstadt University of Technology, **1997**.
[28] a) D. Cremer, J. A. Pople, *J. Am. Chem. Soc.* **1975**, *97*, 1354 – 1358; b) G. A. Jeffrey, R. Taylor, *Carbohydr. Res.* **1980**, *81*, 182 – 183.
[29] a) H. J. Lindner, M. Kroeker, *PIMM91-Closed Shell PI-SCF-LCAO-MO-Molecular Mechanics Program*, Darmstadt University of Technology, **1996**; b) A. E. Smith, H. J. Lindner, *J. Comput.-Aided Mol. Des.* **1991**, *5*, 235 – 262.

Received: March 30, 1999 [F 1709]

  0947-6539/99/0511-3192 $ 17.50+.50/0